Journal of Dental Sciences 19 (2024) 2305–2314

Available online at www.sciencedirect.com

ScienceDirect

journal homepage: www.e-jds.com

Original Article

# Wilms tumor 1-associated protein mediated m6A modification promotes osteogenic differentiation of stem cells from human exfoliated deciduous teeth

Weiheng Gao [a,b], Xixi Miao [b,c], Tao Xu [d*]

[a] Department of Emergency, The Children's Hospital, Zhejiang University School of Medicine, Hangzhou, China
[b] National Clinical Research Center for Child Health, Hangzhou, China
[c] Department of Respiratory Medicine, The Children's Hospital, Zhejiang University School of Medicine, Hangzhou, China
[d] Department of Stomatology, Nanjing Geriatric Hospital, Nanjing, China

Received 16 February 2024; Final revision received 20 February 2024
Available online 24 February 2024

## Introduction

Osteoporosis, trauma, and developmental abnormalities frequently result in the occurrence of alveolar bone defects and inadequate bone mass within the maxillofacial region.[1,2] Consequently, the available choices for oral restoration become limited, often necessitating the use of removable dentures as the primary option to address the absence of alveolar bone.[3] Unfortunately, this approach significantly diminishes both chewing efficiency and retention force. Furthermore, it adversely impacts the success rate of oral implant surgery and necessitates bone grafting procedures to augment bone mass, thereby imposing additional trauma and financial burden on patients. Thus, there is an urgent need to explore more efficient methodologies for enhancing bone growth.[4] Over the past few years, the area of tissue regeneration using stem cells has become a hopeful option for treating bone defects in a clinical setting.[5]

Stem cells from human exfoliated deciduous teeth (SHEDs) have garnered attention due to their capacity for multi-directional differentiation.[6] These cells originate from the pulp stroma of deciduous teeth and exhibit robust osteogenic differentiation and proliferation potential. Notably, when compared to the commonly utilized BMSCs in bone tissue regeneration research, SHEDs offer advantages in terms of accessibility and reduced innate immunogenicity.[7] Consequently, SHEDs are regarded as a viable cell source for bone tissue engineering and regenerative medicine.[8]

N6-methyladenosine ($m^6A$) methylation is the predominant form of RNA modification observed in eukaryotes, constituting more than 60% of all RNA modifications.[9,10] The $m^6A$ modification process encompasses three primary components: writers, erasers, and downstream readers. Writers are responsible for the addition of $m^6A$ to RNA molecules, while erasers dynamically remove $m^6A$ modifications. Downstream readers recognize $m^6A$ and subsequently mediate degradation or stability alterations in the

* Corresponding author. Department of Stomatology, Nanjing Geriatric Hospital, 116 Chengxian Street, Xuanwu District, Nanjing 210018, China.
*E-mail addresses:* 2757224841@qq.com, xutaonanjing@foxmail.com (T. Xu).

https://doi.org/10.1016/j.jds.2024.02.022

associated RNA.[11–13] The m$^6$A Writer protein primarily comprises core constituents METTL3, METTL14, and WTAP, with the identification of additional member proteins such as VIRMA and zc3H13 in recent years.[14] Among these enzyme proteins, WTAP was confirmed to be the third component of methyltransferase. Importantly, WTAP modulates multiple biological functions of stem cells, including pre-mRNA splicing, cell cycle progression and differentiation capacities.[15–17] However, the precise role of WTAP in the osteogenic differentiation process of SHEDs remains uncertain.

This study initially assessed the overall m$^6$A modification level of SHEDs during the process of osteogenic differentiation, along with the expression level of WTAP. Subsequently, we observed that the promotion of osteogenic differentiation in SHEDs is facilitated by WTAP, without any notable impact on cell proliferation. Lastly, we explored the potential role of the RUNX2 gene as a target for WTAP in exerting regulatory effects. Our study elucidates the role of RUNX2 from the perspective of m$^6$A in the osteogenic differentiation of SHEDs, and lays the foundation for the application of WTAP mediated m$^6$A modification in bone tissue regeneration based on SHEDs.

## Materials and methods

### Cell isolation and identification

The separation method of SHEDs refers to published references.[18–20] Briefly, the pulp was initially digested at 37 °C for 30 min in α-MEM (Gibco, Grand Island, NE, USA) supplemented with 3 mg/mL of type I collagenase and 4 mg/mL of trypsin (Gibco). Subsequently, the cells were incubated in α-MEM supplemented with 10% FBS, and 1% streptomycin-penicillin (Gibco) at 37 °C. Flow cytometry was used to detect the expression of MSCs surface markers such as CD29, CD34, CD45, CD90, and CD105.

### Assay for counting cells using cell counting Kit-8

96-well culture plates were used to inoculate SHEDs, which were given 24 h to adhere. After that, the cells were switched to serum-free α-MEM medium and cultured for another 24 h. Following this, the cells were cultured continuously for 0, 1, 3, 5, and 7 days. Each time point, the culture solution was aspirated and CCK-8 solution was added. Subsequently maintained for a duration of 2 h. The absorbance of each well was determined by employing enzyme-linked immunosorbent assay at a wavelength of 450 nm.

### EdU experiment

The SHEDs were immobilized using a 4% paraformaldehyde solution and subsequently treated with 100 μL of a 0.5% TritonX-100 solution for a duration of 10 min. Following this, the samples were exposed to 1 × Apollo staining reaction solution and incubated (darkness, 30 min). Subsequently, 100 μL of 1 × Hoechst 33,342 reaction solution was added and incubated in darkness for another 30 min. The samples were then rinsed with PBS and examined under an inverted fluorescence microscope.

### Alkaline phosphatase and alizarin red staining

Mineralization was initiated once the cell density reached 70%—80%, with the solution being replaced every 3 days. Following a 7-day culture period, SHEDs were immobilized and subjected to ALP staining and quantification using the instructions outlined in the ALP staining kit (Beyotime, Shanghai, China). After a period of 14 days, the presence of mineralized nodules was assessed by employing alizarin red S staining (Beyotime).

### Reverse transcription quantitative polymerase chain reaction (RT-qPCR)

Total RNA was extracted from cells using Trizol for RT-qPCR analysis. Afterward, the entire RNA extracted from cells in every group was transformed into cDNA using reverse transcriptase. The specimens were subjected to preheating at a temperature of 95 °C for a duration of 5 min, followed by heating at 95 °C for 10 s and cooling at 60 °C for 20 s, repeating this process for a total of 55 cycles. PCR amplification was then carried out at 72 °C for 10 s. The resulting CT values were compared for analysis. The primer sequences employed in this study can be found in Table 1.

### Western blot

SHEDs were collected and RIPA buffer was added to extract proteins. Afterwards, electrophoresis was conducted utilizing a 10% SDS-PAGE gel, then transferring onto a PVDF membrane. After sealing the membrane with 5% experimental skimmed milk for 1 h, it was incubated with the primary antibody at 4 °C. The next day, using TBST washed the membrane at room temperature and then incubated with the secondary antibody for 2 h. After TBST washing, the rinsed membrane was placed in an exposure box and exposed to a chemiluminescence substrate for 1 min. Finally, the membrane was appropriately positioned for exposure and imaging.

### Methylated RNA immunoprecipitation

Total RNA was extracted from SHEDS using the TRIzol method. The immunoprecipitation (IP) buffer was incubated for 1 h with either anti-m$^6$A antibodies or anti-IgG antibodies and protein A/G magnetic beads for the purpose of binding. The resulting mRNA and magnetic bead-antibody complexes were then introduced to the IP buffer containing ribonuclease and protease inhibitors, and left to react overnight at 4 °C. The RNA was subsequently eluted using elution buffer and purified through phenol-chloroform extraction.

### RNA stability assay

Samples of SHEDs were collected after being cultured with 5 μg/mL actinomycin D (Sigma, St. Louis, MO, USA). The

**Table 1** The primer sequences used for RT-qPCR.

| Gene | Forward primers (5′-3′) | Reverse primers (5′-3′) |
|---|---|---|
| *WTAP* | TTCCCAAGAAGGTTCGATTG | TGCAGACTCCTGCTGTTGTT |
| *ALP* | GACCTCCTCGGAAGACACTC | TGAAGGGCTTCTTGTCTGTG |
| *RUNX2* | TCTTAGAACAAATTCTGCCCTTT | TGCTTTGGTCTTGAAATCACA |
| *OSX* | CCTCCTCAGCTCACCTTCTC | GTTGGGAGCCCAAATAGAAA |
| *GAPDH* | GGAGCGAGATCCCTCCAAAAT | GGCTGTTGTCATACTTCTCATGG |

total RNA was purified for RT-qPCR, and the mRNA levels of the target genes were compared to the levels of *GAPDH* in order to normalize the data.

### Bone regeneration experiment

This study adhered to the guidelines set forth by the National Institutes of Health and was approved by the Animal Ethics Committee of Nanjing Medical University (IACUC-2108030). The methodology used to construct the model was in line with established techniques outlined in the literature.[21] Briefly, SHEDs infected with OE-NC/OE-WTAP were induced for mineralization over 3 w and subsequently co-cultured with Bio-Oss collagen. Male Sprague–Dawley rats aged 6 weeks (n = 6) were anesthetized, and critical size defects measuring 5 mm were surgically created on both sides of the calvaria. The Bio-Oss collagen scaffold containing cells was then implanted into the defect area. After 8 w, the samples were collected for further studies. The parameter settings for micro-CT and the steps for HE staining are the same as before.[22]

### Statistical analysis

The statistical processing experiments were conducted in triplicate, with the resulting data presented as the mean and standard deviation. The statistical software SPSS 22.0 was employed, utilizing t-tests or one-way ANOVA, and a significance level of $P < 0.05$ was designated as *, indicating a statistically significant difference.

## Results

### The level of m$^6$A modification increased with the osteogenic differentiation of SHEDs

SHEDs were isolated and cultured using the enzyme digestion method. Upon microscopic examination, the primary cells emerged from the dental pulp tissue. Following subculture to the third generation, the cells exhibited typical fibroblast or spindle-like morphology (Fig. 1A). Positive expressions of CD29, CD90, and CD105 were observed in SHEDs by flow cytometry analysis, whereas CD34 and CD45 showed negative results (Fig. 1B). Furthermore, the crystal violet staining demonstrated that SHEDs were capable of forming cell colonies, and the cells displayed a regular spindle shape under high-power microscopy (Fig. 1C). These results indicate that we have successfully isolated and cultured SHEDs.

To elucidate the effect of m$^6$A epigenetic modification on the osteogenic differentiation of SHEDs, SHEDs were induced in mineralization medium firstly. RT-qPCR results revealing a gradual increase of osteogenic differentiation markers (*ALP*, *RUNX2*, and *OSX* ) during the induction process (Fig. 1D). Importantly, quantitative analysis confirmed a concomitant gradual increase in the overall m$^6$A modification level of SHEDs (Fig. 1E). These findings suggest a potential positive role of m$^6$A modification in the osteogenic differentiation of SHEDs.

### Knockdown of WTAP reduces the level of m$^6$A modification and inhibits osteogenic differentiation in SHEDs

Western blot analysis revealed a significant increase in the expression level of WTAP after 7 days of osteogenic induction, which is accompanied by the increase of osteogenic differentiation markers (Fig. 2A and B). Consequently, we hypothesize that WTAP might mediate the m$^6$A modification during the osteogenic differentiation of SHEDs.

To confirm this, we employed siRNA transfection to knockdown the expression level of WTAP in SHEDs, and assessed the efficiency of knockdown using RT-qPCR assay (Fig. 3A). The quantitative analysis of m$^6$A revealed a decrease in the level of m$^6$A modification in SHEDs (Fig. 3B). Besides, the expression levels of RUNX2, OSX, and ALP were decreased through RT-qPCR and Western blot analysis (Fig. 3C and D). Additionally, this trend was supported by the results obtained from ALP and alizarin red staining, as well as quantitative experiments (Fig. 3E and F).

### Overexpression of WTAP up-regulates m$^6$A modification in SHEDS and promotes osteogenic differentiation

To further investigate the role of WTAP-mediated m$^6$A modification in the process of osteogenic differentiation of SHEDs, lentivirus over-expressing WTAP was used to infect SHEDs. The expression of green fluorescence in SHEDs was observed under the inverted fluorescence microscope (Fig. 4A). Besides, the infection efficiency of lentivirus was qualitatively analyzed using RT-qPCR and Western blot (Fig. 4B–D). We observed an increase in the expression levels of osteogenic differentiation markers following WTAP overexpression (Fig. 4E–H). Furthermore, the ALP activity and alizarin red staining in the OE-WTAP group presented significant increase compared to the control group

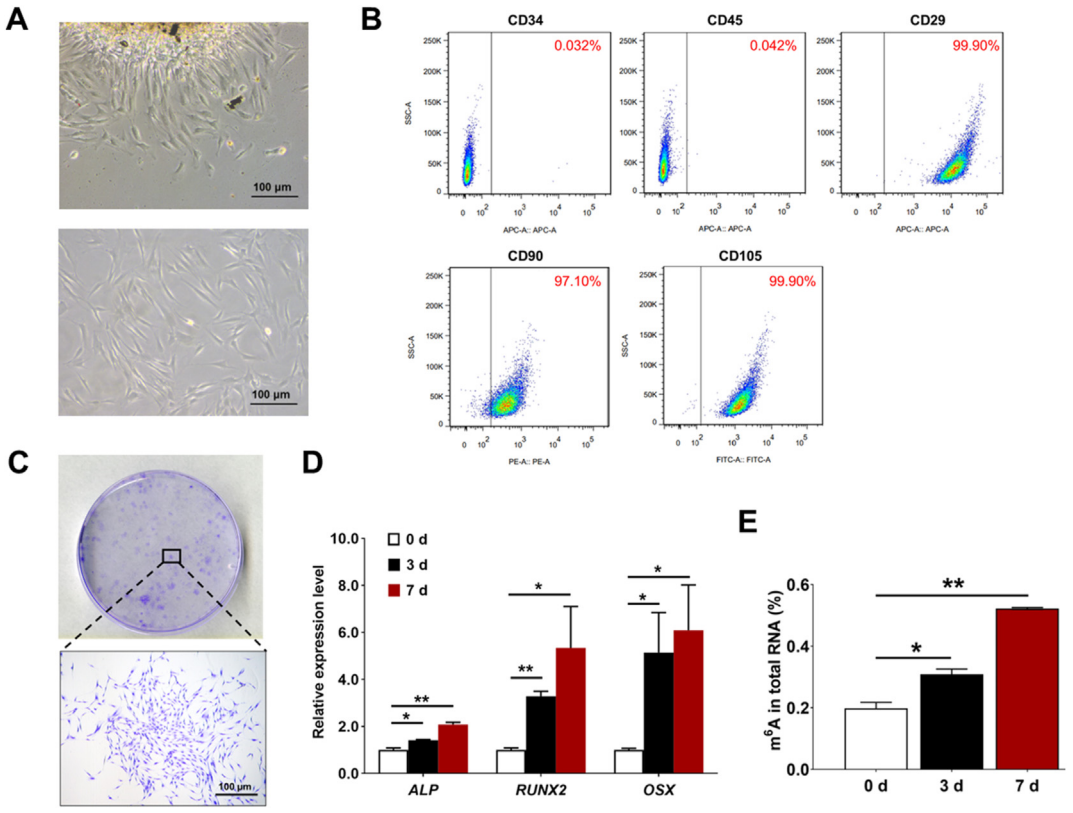


**Figure 1** (A) SHEDs exhibit fibroblast like morphology under the microscope. The above shows the primary generation, and the following shows the P3 cells. (B) Identification of SHEDs by flow cytometry. (C) Observation of self-renewal ability of SHEDs through plate cloning experiment. (D) RT-qPCR detection of expression levels of related markers during cell osteogenic induction process (n = 3). *$P \leq 0.05$, **$P \leq 0.01$ compared to control. (E) M$^6$A activity gradually increases during osteogenic differentiation (n = 3). *$P \leq 0.05$, **$P \leq 0.01$ compared to control.

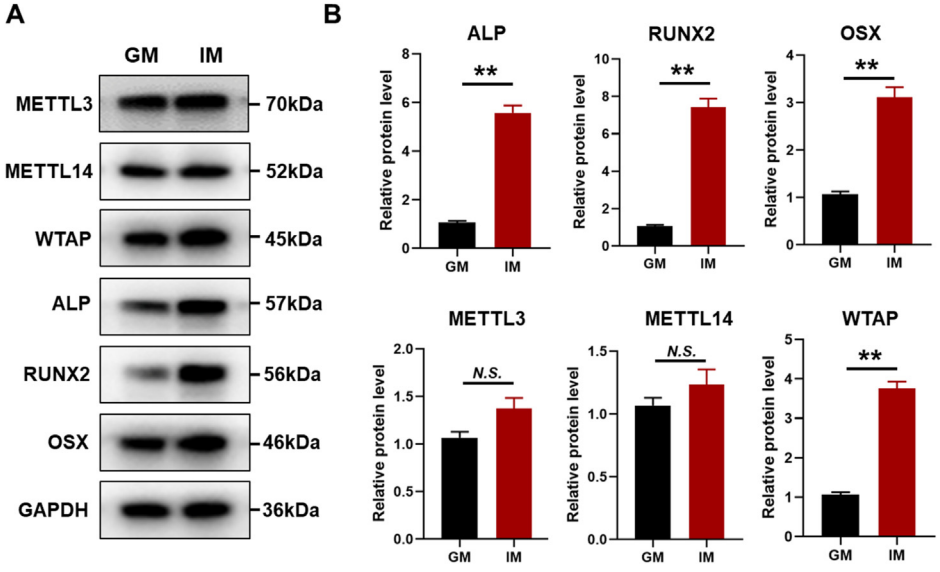


**Figure 2** (A) Detection of expression levels of key m$^6$A methyltransferase in SHEDs after osteogenic differentiation using Western Blot. GM: Growth Medium; IM: Inducing differentiation medium. (B) Quantitative analysis of protein bands in Figure A (n = 3). *$P \leq 0.05$, **$P \leq 0.01$ compared to control; *N.S.*: No significant.

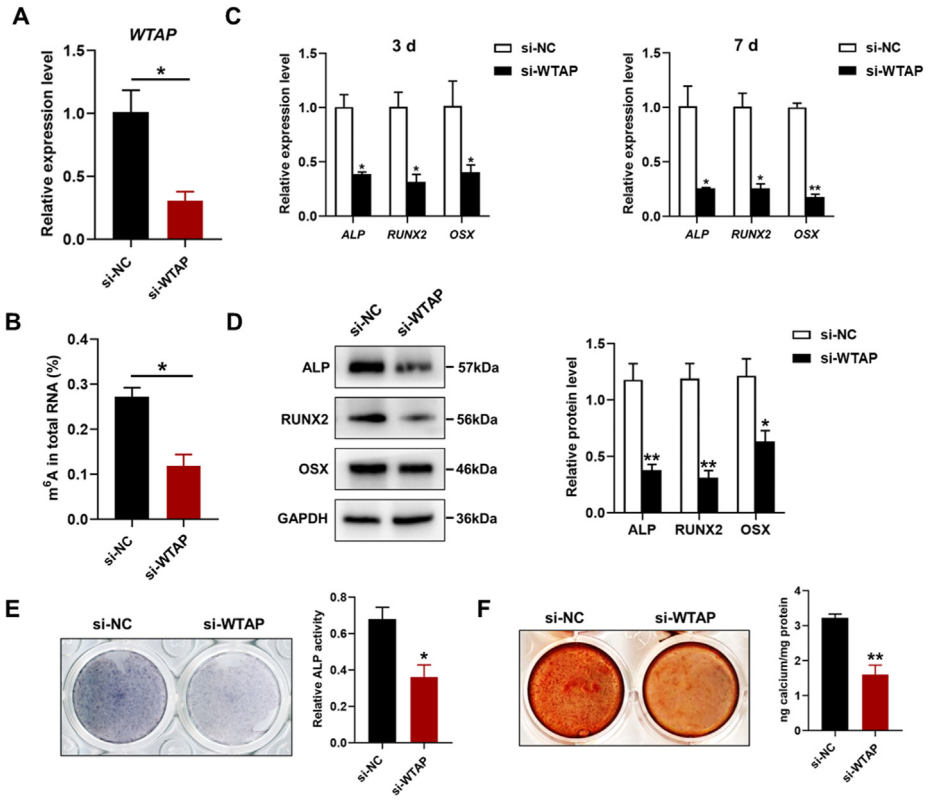


**Figure 3** After knocking down WTAP, the m$^6$A modification level and osteogenic differentiation of SHEDs were inhibited. (A) RT-qPCR detection of transfection efficiency (n = 3). *$P \leq 0.05$ compared to control. (B) The m$^6$A modification level of cells decreases after knocking down WTAP (n = 3). *$P \leq 0.05$ compared to control. (C) RT-qPCR analysis showed that knocking down WTAP resulted in reduced osteogenic differentiation in SHEDs induced for 3 and 7 days, respectively (n = 3). *$P \leq 0.05$, **$P \leq 0.01$ compared to control. (D) After 7 days of induction of osteogenic differentiation in SHEDs, Western Blot testing revealed that knocking down WTAP resulted in reduced osteogenic differentiation (n = 3). *$P \leq 0.05$, **$P \leq 0.01$ compared to control. (E, F) ALP staining, Alizarin Red staining, and corresponding quantitative analysis revealed that knocking down WTAP reduced the deposition of mineralization in SHEDs (n = 3). *$P \leq 0.05$, **$P \leq 0.01$ compared to control. (For interpretation of the references to color in this figure legend, the reader is referred to the Web version of this article.)

(Fig. 4I–K). The results of in vivo experiments found that overexpression of WTAP promotes SHEDs to regenerate bone tissue (Fig. 4L and M). These findings suggest the m$^6$A modification mediated by WTAP could promote the osteogenic differentiation of SHEDs.

## WTAP had no significant effect on the proliferation of SHEDs

The results of EdU suggest that there was no significant alteration in the number of EdU positive cells between the OE-WTAP group and the OE-NC group (Fig. 5A and B). Moreover, the outcomes of CCK-8 experiment also revealed no notable disparity in cell proliferation between the SHEDs in the OE-WTAP group and those in the OE-NC group (Fig. 5C). Collectively, these findings suggest that WTAP does not exert a significant influence on the proliferation of SHEDs.

## RUNX2 is the downstream target gene of WTAP

Previous research has established that the transcription factor RUNX2 plays a crucial role in bone tissue formation. Importantly, utilizing bioinformatics predictions, we have identified 10 potential m$^6$A modification sites on the *RUNX2* that can bind to WTAP. The credibility of 5 of them belongs to the moderate confidence or above, which provides us with the possibility to study the directed differentiation ability of SHEDs regulated by RUNX2 from the perspective of m$^6$A modification (Fig. 6A). To determine whether WTAP directly targets m$^6$A modification on the *RUNX2*, we have designed a gene-specific m$^6$A-qPCR experiment. The findings indicate that the overexpression of WTAP in SHEDs leads to an increase in the enrichment of m$^6$A in *RUNX2* mRNA, as demonstrated in Fig. 6B. Conversely, when the expression of WTAP in SHEDs is reduced, the mRNA stability of *RUNX2* is diminished, as shown in Fig. 6C. Consequently, it can be inferred from these results, as depicted in Fig. 6D, that WTAP has the ability to target *RUNX2* in SHEDs, enhance the *RUNX2* mRNA stability, and facilitate the process of osteogenic differentiation in SHEDs.

## Discussion

The utilization of SHEDs for bone tissue regeneration presents a novel approach for addressing bone defects in

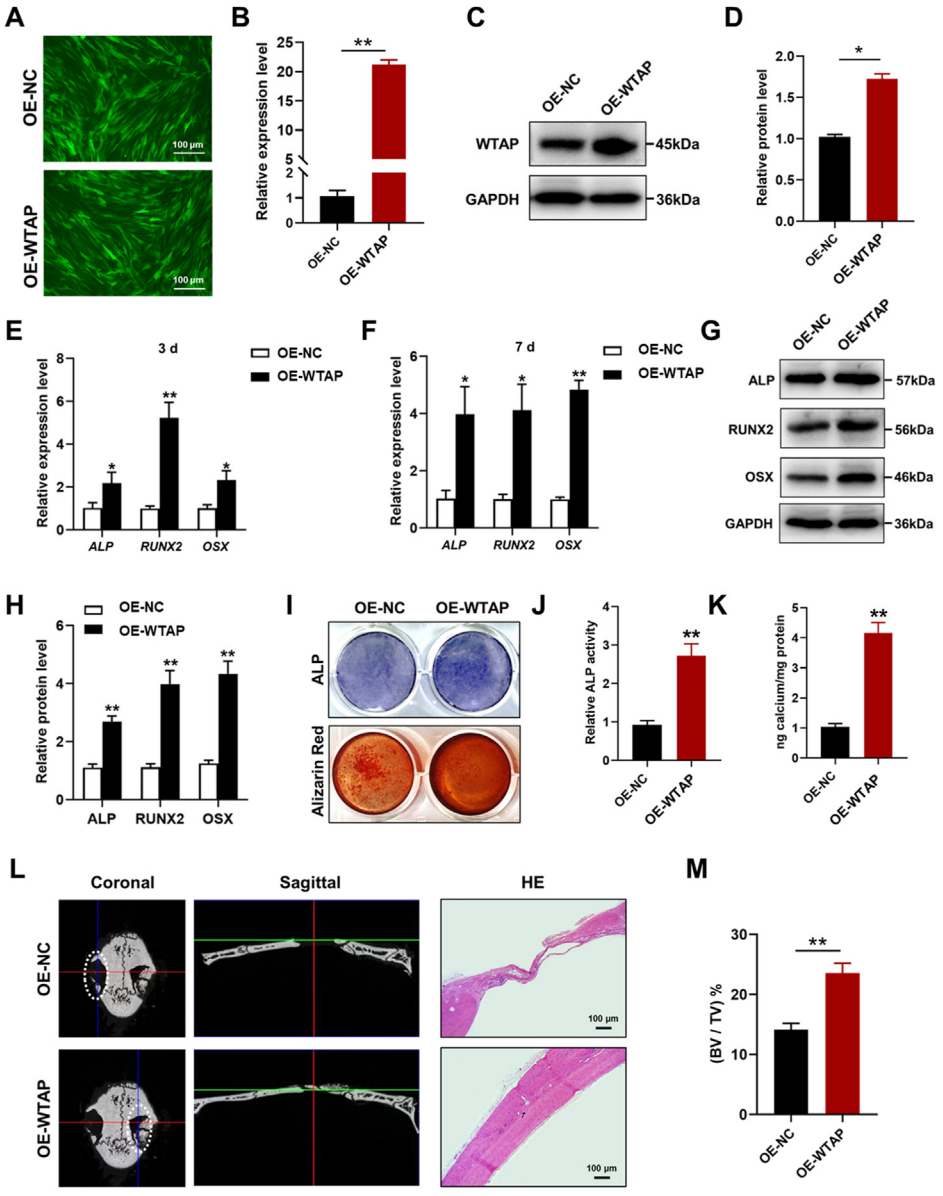


**Figure 4** Overexpression of WTAP promotes osteogenic differentiation of SHEDs. (A) Observation of lentiviral infection efficiency under fluorescence microscopy. (B—D) Efficiency of WTAP overexpression through RT-qPCR and Western Blot assay (n = 3). $^{*}P \leq 0.05$, $^{**}P \leq 0.01$ compared to control. (E, F) The impact of WTAP overexpression on osteogenic differentiation markers was assessed through RT-qPCR after 3 and 7 days of osteogenic induction (n = 3). $^{*}P \leq 0.05$, $^{**}P \leq 0.01$ compared to control. (G, H) Following 7 days of induction, Western Blot analysis demonstrated that overexpression of WTAP led to an upregulation of osteogenic differentiation (n = 3). $^{*}P \leq 0.05$, $^{**}P \leq 0.01$ compared to control. (I—K) ALP staining, Alizarin Red staining, and subsequent quantitative analysis indicated that overexpression of WTAP enhanced mineralization deposition in SHEDs (n = 3). (L) Micro-CT and HE staining confirmed that WTAP promotes bone regeneration in SHEDs in vivo. (M) Bone volume/trabecular volume (BV/TV) was measured in the defect area. $^{*}P \leq 0.05$, $^{**}P \leq 0.01$ compared to control. (For interpretation of the references to color in this figure legend, the reader is referred to the Web version of this article.)

clinical settings, demonstrating promising prospects for application.[23,24] The precise regulation of the biological attributes of SHEDs is crucial for advancing the clinical implementation of bone regeneration facilitated by SHEDs. Herein, we successfully obtained primary human deciduous teeth stem cells. Flow cytometry analysis revealed a high positivity (>97.10%) for mesenchymal stem cell markers (CD29, CD90, CD105). The hematopoietic stem cell markers CD34 and CD45 exhibited negative expression. Furthermore, the cells demonstrated the capacity for colony formation, thereby confirming the successful isolation of SHEDs.

N6-adenylate methylation ($m^6A$) is the predominant RNA modification observed in eukaryotes.[25] Within mammals, the process of RNA $m^6A$ modification is facilitated by a methyltransferase complex known as "writers", which

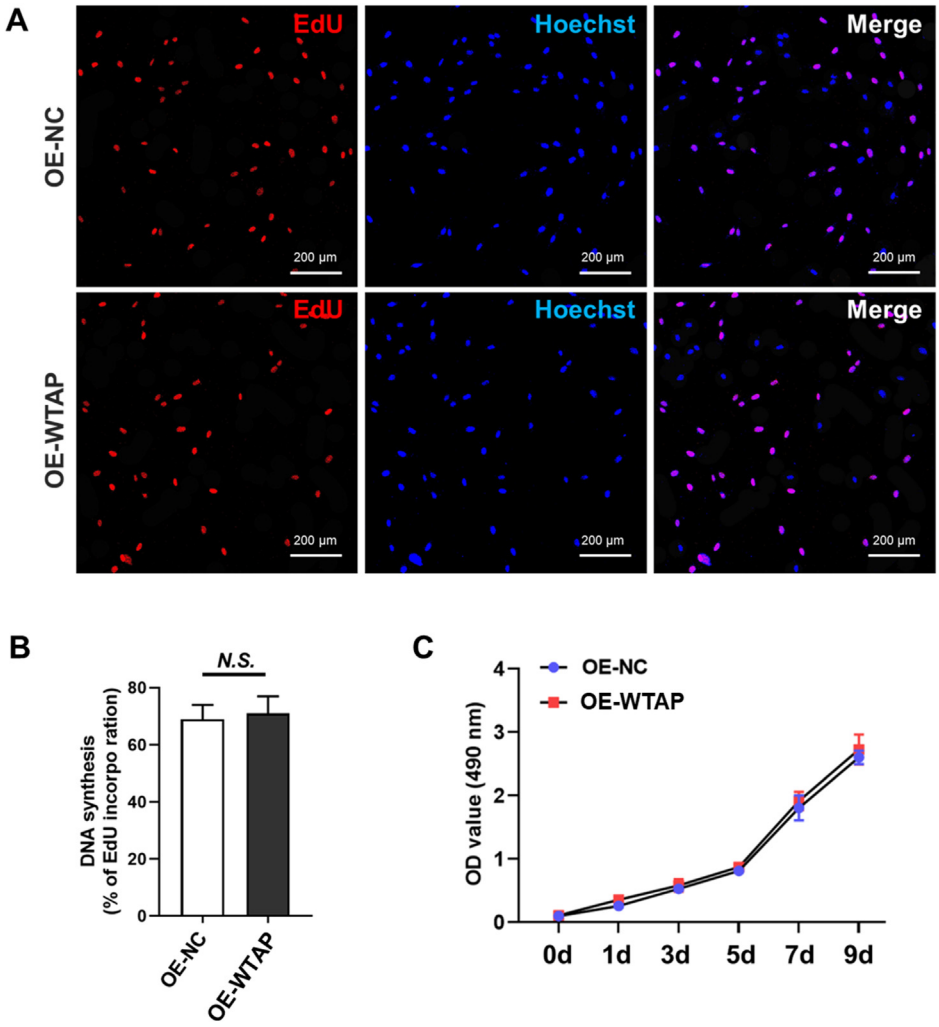


**Figure 5** WTAP has no significant effect on the proliferation ability of SHEDs. (A, B) EdU assay found that there was no significant change in the proliferation ability of SHEDs in the WTAP overexpression group compared to the control group. (C) The CCK-8 test found that compared to the control group. There was no difference in the proliferation ability of WTAP group cells at different time points.

consists of three essential components: the catalytic factor METTL3, the substrate METTL14, and the associated protein WTAP.[26,27] Recent studies have found that WTAP increases the DNA methylation level of pri-miR-181a in BMSCs, subsequently enhancing its transformation into mature miRNA and facilitating osteogenesis. Furthermore, WTAP is capable of augmenting the expression of miR-29 b-3p via $m^6A$ modification, consequently amplifying the osteogenic potential of these BMSCs in individuals with osteoporosis.[28,29] In this study, we induced SHEDs osteogenic differentiation firstly and assessed the expression levels of key methyltransferase enzymes using Western blot. Our findings revealed a significant increase in the expression level of WTAP, suggesting that WTAP may play a role in promoting osteogenic differentiation of SHEDs.

To validate this hypothesis, the successful transfection of si-WTAP was confirmed through RT-qPCR. Subsequently, under osteogenic induction conditions, the RT-qPCR results at 7 and 14 days indicated a downward trend in the expression levels of osteogenic differentiation markers in the si-WTAP group compared to the control group. This suggests that WTAP might promote the committed differentiation of SHEDs. Western blot analysis further substantiated this finding. Furthermore, the results obtained from ALP staining, activity detection, and alizarin red staining indicate a diminished mineralization capacity of SHEDs in the si-WTAP group. Notably, a concurrent decrease in $m^6A$ level was observed. Conversely, when SHEDs were infected with WTAP overexpression lentivirus, an opposing trend was observed. Recent research has highlighted the osteogenic differentiation-promoting effects of WTAP on BMSCs and its potential to mitigate estrogen deficiency-induced bone loss.[30] This is similar to the result of WTAP promoting the directional differentiation of SHEDs found in this study.

The EdU and CCK-8 results showed no significant difference in the proliferation activity of SHEDs between the OE-WTAP group and the control group. This suggests that WTAP does not exert an influence on the proliferation of SHEDs. In contrast, previous studies reported that WTAP facilitates the proliferation of osteosarcoma cells.[31,32] We

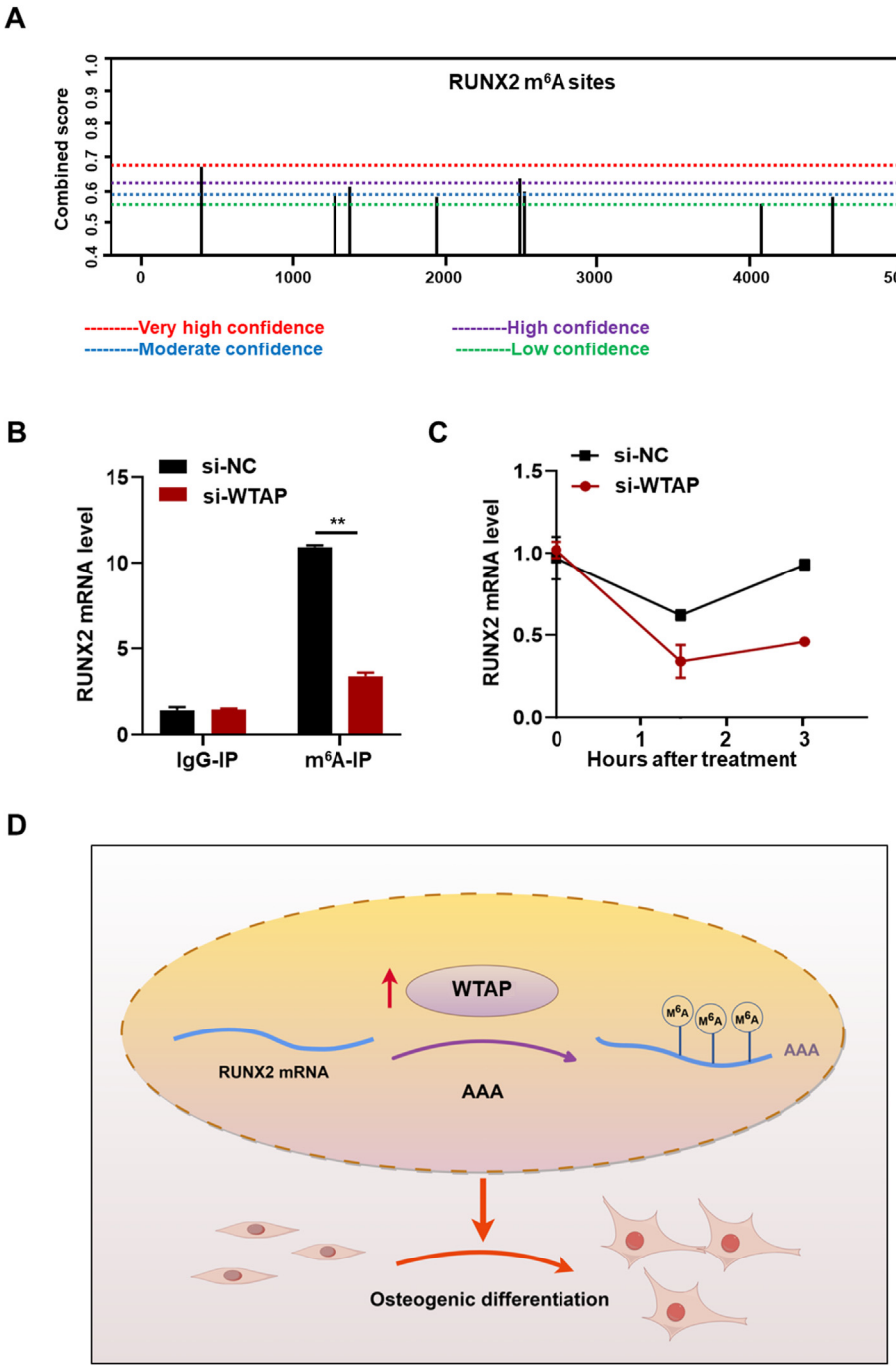


**Figure 6** *RUNX2* is a downstream target gene for WTAP mediated m$^6$A modification to regulate SHEDs directional differentiation. (A) Predicting potential modification sites on the *RUNX2* gene through bioinformatics. (B) The m$^6$A-IP experiment confirmed that WTAP can target and modify *RUNX2* (n = 3). $^{**}P \leq 0.01$ compared to control. (C) The actinomycin D experiment found that WTAP mediated m$^6$A modification can enhance the gene stability of *RUNX2*. (D) The mechanism diagram of this study.

postulate that this discrepancy may arise from the distinct regulatory roles of WTAP in the proliferation mechanisms of various cell lines.

In terms of its effect on RNA metabolism, m$^6$A mainly influences mRNA translation, mRNA splicing, mRNA nuclear export, and mRNA stability.[33–36] The present investigation primarily concentrates on mRNA stability, as modifications to mRNA decay significantly influence the abundance of cellular mRNA. It is widely recognized that *RUNX2* serves as an early osteogenic differentiation marker gene, and numerous studies have substantiated its role in the osteogenic differentiation of SHEDs.[37,38] This study is significant as it marks the first exploration of WTAP-mediated RUNX2 m$^6$A modification in the directional differentiation of SHEDs, focusing on the aspect of m$^6$A epigenetic modification. The findings of this study contribute to the existing

knowledge on the pathway of RUNX2 as a transcription factor in the osteogenic differentiation of SHEDs.

In summary, the findings of this study demonstrate that the WTAP gene has the ability to enhance the osteogenic differentiation of SHEDs. Consequently, the utilization of WTAP-modified SHEDs presents a novel avenue for investigating bone regeneration.

## Declaration of competing interest

The authors have no conflicts of interest relevant to this article.

## Acknowledgement

This research was supported by Nanjing medical science and technology development fund (YKK22201).

## References

1. Everts-Graber J, Lehmann D, Burkard JP, et al. Risk of osteonecrosis of the jaw under denosumab compared to bisphosphonates in patients with osteoporosis. *J Bone Miner Res* 2022;37:340—8.
2. Tiwary P, Sahoo N, Thakral A, Ranjan U. Styloid process fracture associated with maxillofacial trauma: incidence, distribution, and management. *J Oral Maxillofac Surg* 2017;75:2177—82.
3. Monje A, Roccuzzo A, Buser D, Wang HL. Influence of buccal bone wall thickness on the peri-implant hard and soft tissue dimensional changes: a systematic review. *Clin Oral Implants Res* 2023;34(Suppl 26):8—27.
4. Li Z, Yan M, Yu Y, et al. LncRNA H19 promotes the committed differentiation of stem cells from apical papilla via miR-141/SPAG9 pathway. *Cell Death Dis* 2019;10:130.
5. Lu G, Xu Y, Liu Q, et al. An instantly fixable and self-adaptive scaffold for skull regeneration by autologous stem cell recruitment and angiogenesis. *Nat Commun* 2022;13:2499.
6. Shi X, Mao J, Liu Y. Pulp stem cells derived from human permanent and deciduous teeth: biological characteristics and therapeutic applications. *Stem Cells Transl Med* 2020;9:445—64.
7. Guo R, Gu T, Xiao Y, et al. Hsa-miR-27b-5p suppresses the osteogenic and odontogenic differentiation of stem cells from human exfoliated deciduous teeth via targeting BMPR1A: an ex vivo study. *Int Endod J* 2023;56:1284—300.
8. Guo R, Fang Y, Zhang Y, et al. SHED-derived exosomes attenuate trigeminal neuralgia after CCI of the infraorbital nerve in mice via the miR-24-3p/IL-1R1/p-p38 MAPK pathway. *J Nanobiotechnol* 2023;21:458.
9. Huang M, Xu S, Liu L, et al. M6A methylation regulates osteoblastic differentiation and bone remodeling. *Front Cell Dev Biol* 2021;9:783322.
10. Xu Y, Liu W, Ren L. Emerging roles and mechanism of m6A methylation in rheumatoid arthritis. *Biomed Pharmacother* 2024;170:116066.
11. Shi H, Wei J, He C. Where, when, and how: context-dependent functions of RNA methylation writers, readers, and erasers. *Mol Cell* 2019;74:640—50.
12. Roundtree IA, Evans ME, Pan T, He C. Dynamic RNA modifications in gene expression regulation. *Cell* 2017;169:1187—200.
13. Wang P, Xie D, Xiao T, et al. H3K18 lactylation promotes the progression of arsenite-related idiopathic pulmonary fibrosis via YTHDF1/m6A/NREP. *J Hazard Mater* 2024;461:132582.
14. He PC, He C. m(6A RNA methylation: from mechanisms to therapeutic potential. *EMBO J* 2021;40:e105977.
15. Chen J, Zhang H, Xiu C, et al. METTL3 promotes pancreatic cancer proliferation and stemness by increasing stability of ID2 mRNA in a m6A-dependent manner. *Cancer Lett* 2023;565:216222.
16. Yang X, Mei C, Raza SHA, et al. Interactive regulation of DNA demethylase gene TET1 and m(6)A methyltransferase gene METTL3 in myoblast differentiation. *Int J Biol Macromol* 2022;223:916—30.
17. Yang Y, Zeng J, Jiang C, et al. METTL3-mediated lncSNHG7 m(6)A modification in the osteogenic/odontogenic differentiation of human dental stem cells. *J Clin Med* 2022;12:113.
18. Ivan A, Cristea MI, Telea A, et al. Stem cells derived from human exfoliated deciduous teeth functional assessment: exploring the changes of free fatty acids composition during cultivation. *Int J Mol Sci* 2023;24:17249.
19. Hiraki T, Kunimatsu R, Nakajima K, et al. Stem cell-derived conditioned media from human exfoliated deciduous teeth promote bone regeneration. *Oral Dis* 2020;26:381—90.
20. Chen G, Tu Y, Aladelusi TO, et al. Knocking down B7H3 expression enhances cell proliferation of SHEDs via the SHP1/AKT signal axis. *Biochem Biophys Res Commun* 2020;531:282—9.
21. Xiao Y, Chen L, Xu Y, et al. Circ-ZNF236 mediates stem cells from apical papilla differentiation by regulating LGR4-induced autophagy. *Int Endod J* 2024 (in press).
22. Xu T, Wu X, Zhou Z, et al. Hyperoside ameliorates periodontitis in rats by promoting osteogenic differentiation of BMSCs via activation of the NF-kappaB pathway. *FEBS Open Bio* 2020;10:1843—55.
23. Kunimatsu R, Rikitake K, Yoshimi Y, Putranti NaR, Hayashi Y, Tanimoto K. Bone differentiation ability of CD146-positive stem cells from human exfoliated deciduous teeth. *Int J Mol Sci* 2023;24:4048.
24. Hara K, Yamada Y, Nakamura S, Umemura E, Ito K, Ueda M. Potential characteristics of stem cells from human exfoliated deciduous teeth compared with bone marrow-derived mesenchymal stem cells for mineralized tissue-forming cell biology. *J Endod* 2011;37:1647—52.
25. Yang Y, Hsu PJ, Chen YS, Yang YG. Dynamic transcriptomic m(6)A decoration: writers, erasers, readers and functions in RNA metabolism. *Cell Res* 2018;28:616—24.
26. Cheng C, Zhang H, Zheng J, Jin Y, Wang D, Dai Z. METTL14 benefits the mesenchymal stem cells in patients with steroid-associated osteonecrosis of the femoral head by regulating the m6A level of PTPN6. *Aging (Albany NY)* 2021;13:25903—19.
27. Bai Y, Jiao X, Hu J, Xue W, Zhou Z, Wang W. WTAP promotes macrophage recruitment and increases VEGF secretion via N6-methyladenosine modification in corneal neovascularization. *Biochim Biophys Acta, Mol Basis Dis* 2023;1869:166708.
28. You Y, Liu J, Zhang L, et al. WTAP-mediated m(6)A modification modulates bone marrow mesenchymal stem cells differentiation potential and osteoporosis. *Cell Death Dis* 2023;14:33.
29. Liu J, You Y, Sun Z, et al. WTAP-mediated m6A RNA methylation regulates the differentiation of bone marrow mesenchymal stem cells via the miR-29b-3p/HDAC4 axis. *Stem Cells Transl Med* 2023;12:307—21.
30. Yan G, Yuan Y, He M, et al. M(6)A methylation of precursor-miR-320/RUNX2 controls osteogenic potential of bone marrow-derived mesenchymal stem cells. *Mol Ther Nucleic Acids* 2020;19:421—36.
31. Han J, Wang JZ, Yang X, et al. METTL3 promote tumor proliferation of bladder cancer by accelerating pri-miR221/222 maturation in m6A-dependent manner. *Mol Cancer* 2019;18:110.
32. Xu Y, Bao Y, Qiu G, Ye H, He M, Wei X. METTL3 promotes proliferation and migration of colorectal cancer cells by increasing SNHG1 stability. *Mol Med Rep* 2023;28:217.

33. Qiao Y, Sun Q, Chen X, et al. Nuclear m6A reader YTHDC1 promotes muscle stem cell activation/proliferation by regulating mRNA splicing and nuclear export. *Elife* 2023;12: e82703.
34. Wen J, Lv R, Ma H, et al. Zc3h13 regulates nuclear RNA m(6)A methylation and mouse embryonic stem cell self-renewal. *Mol Cell* 2018;69:1028—10238 e6.
35. Berulava T, Buchholz E, Elerdashvili V, et al. Changes in m6A RNA methylation contribute to heart failure progression by modulating translation. *Eur J Heart Fail* 2020;22:54—66.
36. Uzonyi A, Dierks D, Nir R, et al. Exclusion of m6A from splice-site proximal regions by the exon junction complex dictates m6A topologies and mRNA stability. *Mol Cell* 2023;83:237—251 e7.
37. Zhang N, Chen B, Wang W, et al. Isolation, characterization and multi-lineage differentiation of stem cells from human exfoliated deciduous teeth. *Mol Med Rep* 2016;14:95—102.
38. Zhu Z, Huang F, Xia W, et al. Osteogenic differentiation of renal interstitial fibroblasts promoted by lncRNA MALAT1 may partially contribute to Randall's plaque formation. *Front Cell Dev Biol* 2020;8:596363.